

9.9.1963

CHARGED SIGMA HYPERON LEPTONIC DECAYS \*

H. Courant,<sup>(a)</sup> H. Filthuth, R.G. Glasser,<sup>(b)</sup>  
A. Minguzzi-Ranzi, A. Segar,<sup>(c)</sup> W. Willis,<sup>(d)</sup>

CERN, Geneva, Switzerland

R.A. Burnstein, T.B. Day, A.J. Herz, B. Kehoe  
B. Sechi-Zorn, N. Seeman, G.A. Snow,<sup>(e)</sup>

University of Maryland, College Park, Maryland, and  
U.S. Naval Research Laboratory, Washington, D.C.

\* Work at University of Maryland supported by U.S. Atomic Energy Commission.

- (a) Ford Fellow (CERN) 1961-1962, U.S. National Science Foundation Senior Post-Doctoral Fellow 1962-1963.
- (b) U.S. National Science Foundation Senior Post-Doctoral Fellow on leave from U.S. Naval Research Laboratory.
- (c) N.I.R.N.S., Chilton, England.
- (d) Ford Fellow (CERN) 1961-1962, present address: Brookhaven National Laboratory.
- (e) U.S. National Science Foundation Senior Post-Doctoral Fellow at CERN, 1961-1962.

100-100000-100000

100-100000-100000

100-100000-100000

100-100000-100000

100-100000-100000

100-100000-100000

100-100000-100000

100-100000-100000

100-100000-100000

100-100000-100000

100-100000-100000

100-100000-100000

100-100000-100000

100-100000-100000

100-100000-100000

100-100000-100000

100-100000-100000

100-100000-100000

100-100000-100000

100-100000-100000

100-100000-100000

100-100000-100000

100-100000-100000

100-100000-100000

100-100000-100000

100-100000-100000

100-100000-100000

100-100000-100000

100-100000-100000

100-100000-100000

100-100000-100000

100-100000-100000

100-100000-100000

100-100000-100000

100-100000-100000

100-100000-100000

100-100000-100000

100-100000-100000

100-100000-100000

100-100000-100000

100-100000-100000

100-100000-100000

100-100000-100000

100-100000-100000

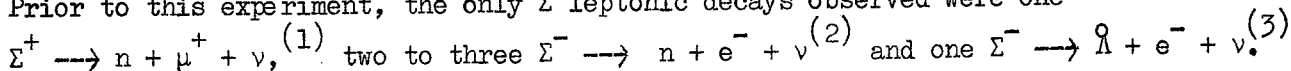
- 1 -

We have examined the CERN stopping  $K^-$  film for the following decays.



produced in the reaction  $K^- + p \longrightarrow \Sigma^+ + \pi^-$  ( $K^-$  at rest).

Prior to this experiment, the only  $\Sigma$  leptonic decays observed were one



This report is based on the observation of about hundred  $\Sigma$  leptonic decays.

(i)  $\Sigma^+ \longrightarrow n + \mu^+ + \nu$  decays - About  $1.6 \cdot 10^5$  pictures containing  $6 \times 10^5$   $K^-$  mesons were scanned for these decay modes.

The film was scanned in two views, with the third view available. All ( $K^-, p$ ) at rest events (i.e. co-linear  $\Sigma\pi$ ) were examined, and the secondary from the  $\Sigma$  decay measured with a curvature template. The dip was estimated on the scanning table, and all events with curvature corresponding to a momentum  $< 110$  MeV/c and a dip angle  $< 60^\circ$  were measured with standard digitized measuring machines. The dip criterion was not applied if the decay secondary stopped in the chamber.

The reconstruction and fitting program gave data on the secondary assuming in turn that it was a pion, muon or electron. The kinematic fitting was carried out in two parts. First the ( $K^-, p$ ) production vertex was tested and retained in our sample if this vertex was consistent with a zero energy  $K^-$  reaction. Secondly the fitted  $\Sigma^+$  from production was combined with the measurements of the decay track assuming it to be a  $\mu^+$  to test the  $\Sigma^+ \longrightarrow \mu^+ + n$  hypothesis. Any event which fit the  $\pi$  decay with confidence greater than 0.01 percent was rejected as a possible leptonic decay. In addition it was required that the  $\Sigma^+$  and  $\Sigma^-$  have a length  $> 1$  mm and that the  $\Sigma^-$  have a residual range at the point of decay  $> 1$  mm.

The remaining candidates were then re-examined by physicists. From an estimate of the bubble density of each secondary track, it was always possible to distinguish pions or muons from electrons. Special attention was given to the possible muons to eliminate the  $\pi - \mu$  decay background. Events were eliminated if either the secondary track had a visible kink or if its momentum and angle in the laboratory with respect to the sigma direction was such that it could have arisen kinematically from a  $\Sigma \rightarrow \pi n$ ,  $\pi \rightarrow \mu$  decay.

1. The first part of the document discusses the importance of maintaining accurate records of all transactions. It emphasizes that proper record-keeping is essential for the integrity of the financial system and for the ability to detect and prevent fraud.

2. The second part of the document outlines the various methods used to collect and analyze data. It describes the process of gathering information from different sources and how this data is then processed to identify trends and anomalies. This section also discusses the role of technology in modern data analysis.

3. The third part of the document focuses on the application of statistical techniques to financial data. It explains how statistical models can be used to predict future trends and to assess the risk of various investments. This part also covers the importance of understanding the limitations of these models and the need for ongoing monitoring and adjustment.

4. The final part of the document discusses the ethical considerations surrounding financial data analysis. It highlights the need for transparency and accountability in the use of data and the importance of protecting individual privacy. It also touches on the broader implications of data analysis for society and the economy.

- 2 -

34  $\Sigma^-$  decays and 1  $\Sigma^+$  decay satisfying these criteria were found. 18  $\mu^-$  decayed at rest into electrons so that in this subset the distinction between muons and pions was certain. An alternate explanation of the remaining 16  $\Sigma^-$  events and 1  $\Sigma^+$  event can be the radiative decay  $\Sigma^\pm \rightarrow n + \pi^\pm + \gamma$ .<sup>(4)</sup> It is probable that most of these events are  $\mu$  decays however, since we have seen only 2 stopping  $\pi^+$  and 1 stopping  $\pi^-$  from this type of decay in our sample<sup>(4a)</sup>.

Figure 1 displays a histogram of the momentum distribution of the 34 observed  $\mu^-$  events. The 18 events where the  $\mu^-$  stops in the chamber are cross-hatched. The upper smooth curve represents the theoretical momentum spectrum for the  $\mu^-$ .<sup>(5)</sup>

The lower smooth curve represents the calculated probability of obtaining stopping  $\mu^-$  events in the Saclay 81 cm chamber<sup>(6)</sup> multiplied by the phase space distribution transformed to the laboratory system. The fraction of all  $\mu^-$  that stop in the chamber turns out to be 0.12. As one final correction, we estimate that our scanning efficiency for finding stopping  $\mu^-$  events is 90 percent. We use only the stopping event to determine the  $(\Sigma^- \rightarrow n + \mu^- + \nu^-)/(\Sigma^- \rightarrow n + \pi^-)$  branching ratio,  $R_-(\mu)$ .

The number of  $\Sigma^- \rightarrow n + \pi^-$  decays needed to determine  $R_-(\mu)$  is obtained as follows. The number of  $\Lambda^0 + e^- + e^+$  events from  $K^-$  endings is 2800 in this sample of film. Using the data of Humphrey and Ross<sup>(7)</sup> for the relative production rate of  $\Sigma^0 \pi^0$ ,  $\Lambda^0 \pi^0$ ,  $\Sigma^- \pi^+$  and  $\Sigma^+ \pi^-$  from  $(K^-, p)$  captures, one deduces the number of  $K^-$  captures at rest to be  $6 \times 10^5$ . The effective number of  $(\Sigma^- \rightarrow \pi^- + n)$  decays is obtained by reducing the number of  $\Sigma^-$  produced ( $2.75 \times 10^5$ ) by 13 percent for the number that decay in less than 1 mm and by 18 percent for the number of  $\Sigma^-$  with residual range of 1 mm or less. We get  $1.90 \times 10^5$  effective  $\Sigma^- \rightarrow \pi^- + n$  decays. An analogous estimate yields  $0.47 \times 10^5$   $\Sigma^+ \rightarrow \pi^+ + n$  decays. Finally the 18 stopping  $\mu^-$  events yield

$$R_-(\mu) = \frac{\Sigma^- \rightarrow \mu^- + n + \nu^-}{\Sigma^- \rightarrow \pi^- + n} = (8.8 \pm 3.0) \times 10^{-4} \quad (2)$$

The universal Fermi interaction (UFI) hypothesis predicts that  $R_-(\mu)$  is 2.6 percent. This experiment confirms again<sup>(2)</sup> that the strangeness changing leptonic decays of hyperons is smaller by more than an order of magnitude than the UFI prediction. The ratio UFI prediction/Experiment =  $30 \pm 8$  for  $\Sigma^- \rightarrow \mu^- + n + \nu$  decays is similar to the ratio  $20 \pm 3$  found for  $\Lambda^0 \rightarrow p + e^- + \nu$  decays by Ely et al.<sup>(8)</sup>

The first part of the document discusses the importance of maintaining accurate records of all transactions. It emphasizes that every entry should be supported by a valid receipt or invoice. This ensures transparency and allows for easy verification of the data.

In the second section, the author details the various methods used to collect and analyze the data. This includes both manual and automated processes. The manual process involves reviewing each entry individually, while the automated process uses software to identify patterns and anomalies.

The third section describes the results of the analysis. It shows that there are several areas where the data is inconsistent or incomplete. These areas need to be investigated further to determine the cause of the discrepancies.

Finally, the document concludes with a list of recommendations. These include implementing stricter controls over data entry, improving the accuracy of the automated systems, and conducting regular audits to ensure the integrity of the data.

- 3 -

The one  $\Sigma^+$  event satisfying our criteria had a secondary of initial momentum  $86.7 \pm 2.6$  MeV/c or  $90.0 \pm 2.7$  MeV/c for a  $\mu^+$  or  $\pi^+$  respectively. There is no evidence of  $\pi - \mu$  decay or anomalous scattering along all of its length (24.4 cm)<sup>(9)</sup>. At the decay point the  $\Sigma^+$  hyperon has a momentum of 175 MeV/c and the decay angle is  $74^\circ$ . At this angle, a muon arising from the chain  $\Sigma^+ \rightarrow \pi^+ + n$ ,  $\pi^+ \rightarrow \mu^+ + \nu$  must have  $P_\mu \gtrsim 99$  MeV/c. Furthermore this would require a  $\pi^+ \rightarrow \mu^+ + \nu$  decay in a small solid angle near the backward direction in the first few millimeters of the pion track. Hence this interpretation of the event is extremely improbable.

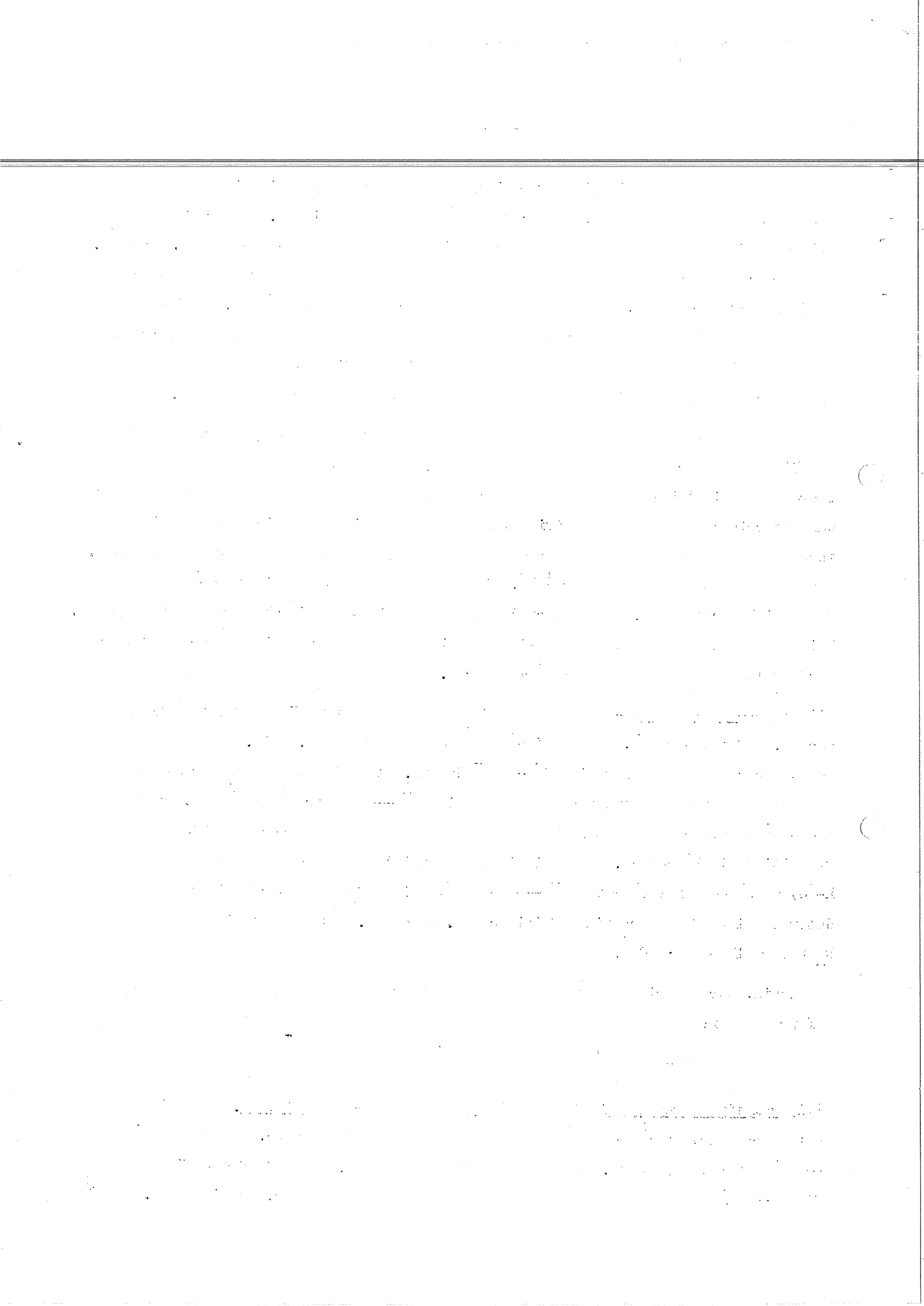
A small delta ray was found on the secondary track at a point where the momentum was 71 or 75 MeV/c for a  $\mu$  or a  $\pi$  respectively. The energy of this delta ray from range (2 mm) is  $148 \pm 5$  kev. The angle between this delta ray and the positive track was determined by measuring individual bubbles under high magnification and fitting these measurements with a reconstruction routine which took into account energy loss. The angle was measured to be  $29 \pm 5^\circ$ , with an additional uncertainty of  $\pm 11^\circ$  due to multiple scattering. The expected value for  $\pi^+$  is  $40^\circ \pm 3^\circ$  and for a  $\mu^+$  is  $51 \pm 3^\circ$ . This result favours the interpretation of this event as a radiative  $\Sigma^+ \rightarrow n + \pi^+ + \gamma$  decay rather than a  $\Sigma^+ \rightarrow n + \mu^+ + \nu$  decay.

(ii)  $\Sigma^+ \rightarrow n + e^+ + \nu$  - In the same film we have observed 70  $e^-$  and 3  $e^+$  from  $\Sigma$  decays. Of these 25  $e^-$ , and all 3  $e^+$  have momenta  $< 60$  MeV/c. Fig. 2 shows the momentum spectrum of the negative  $\Sigma^- \rightarrow e^-$  decays. In this low momentum region, events are ambiguous between the two categories  $\Sigma^- \rightarrow (n \text{ or } \Lambda^0) + e^\pm + \nu$ , so that the 3  $e^+$  events cannot be taken as demonstration of the existence of  $(\Delta S/\Delta Q) = -1$  transitions in  $\Sigma^+$  decays. The principal uncertainty in evaluating  $R_-(e) = R_-(e) = (\Sigma^- \rightarrow n + e^- + \nu / \Sigma^- \rightarrow n + \pi^-)$  arises from the uncertainty in our determination of the scanning efficiency vs. momentum. Our best estimate is  $R_-(e) = (13 \pm 4) \cdot 10^{-4}$ .

Again, our experimental value is suppressed by a large factor relative to the UFI production:

$$R_-(e) \text{ UFI} / R_-(e) \text{ Experiment} = 45 \begin{matrix} + 10 \\ - 11 \end{matrix}$$

(iii) Relative strength of  $(\Delta S/\Delta Q) = +1$  and  $(\Delta S/\Delta Q) = -1$  transitions. Assuming that we can neglect  $\Sigma^\pm \rightarrow \Lambda^0 + e^\pm + \nu$  decays for  $P_e < 60$  MeV/c, we have 45  $\Sigma^- \rightarrow e^- + n + \nu$  events vs. 0  $\Sigma^+ \rightarrow e^+ + n + \nu$  events. The "effective" number of  $\Sigma^- \rightarrow \pi^- + n$  and  $\Sigma^+ \rightarrow \pi^+ + n$  decays in this sample is  $19.0 \times 10^4$  and  $4.7 \times 10^4$





- 4 -

respectively. Hence

$$\rho(e) = \frac{\text{Rate of } (\Sigma^+ \rightarrow e^+ + n + \nu)}{\text{Rate of } (\Sigma^- \rightarrow e^- + n + \nu)} = \left(\frac{0}{45}\right) \times \left(\frac{19.0}{4.7}\right) = \frac{0}{11.1}$$

To study  $\Delta S/\Delta Q = \pm 1$  transitions in the  $\Sigma \rightarrow \mu + n + \nu$  decay, we have to be certain in identifying the secondary as a  $\mu$ -meson. This is only possible if the  $\mu$ -meson comes to rest inside the bubble chamber. We have found 20  $\Sigma^-$  - events, where the  $\mu^-$  - secondaries decayed at rest into electrons and no such  $\Sigma^+$  decay. Consequently

$$\rho(\mu) = \frac{0}{20} \cdot \frac{13}{4.7} = \frac{0}{4.8}$$

Assuming that  $\rho(e) = \rho(\mu)$ , the 90 o/o confidence limit is

$$\rho = \frac{\text{rate of } (\Delta S/\Delta Q) = -1 \text{ transitions}}{\text{rate of } (\Delta S/\Delta Q) = +1 \text{ transitions}} = \frac{2.3}{15.9} < 0.14 \quad (3)$$

(iv)  $\Sigma^+ \rightarrow \Lambda^0 + e^+ + \nu$  - The ratio of rates of  $\Sigma^+ \rightarrow \Lambda^0 + e^+ + \nu$  to  $\Sigma^- \rightarrow \Lambda^0 + e^- + \nu$  is predicted to be 0.60 if the  $\Sigma\Lambda$  current is pure I = 1<sup>(10)</sup> (that is, hyperon currents of the first kind only, in the language of Weinberg<sup>(11)</sup>). If the  $\Delta S = 0$  ( $\Sigma\Lambda$ ) current is closely related to ordinary beta decay, one can hypothesize that the vector current is conserved, so that it makes no contribution to these decays, and one can estimate the rate of allowed axial vector decay by using a Goldberger Treiman relation and the UFI hypothesis<sup>(12)</sup>. This yields

$$R_{\Lambda^-} = \frac{\Sigma^- \rightarrow \Lambda^0 + e^- + \nu}{\Sigma^- \rightarrow n + \pi^-} = 1.3 \times 10^{-4} (f_{\Sigma\Lambda\pi}/f_{pp\pi})^2 = 1.0 \times 10^{-4}$$

Where we have used  $(f_{\Sigma\Lambda\pi}/f_{pp\pi})^2 = 0.80$  from the analysis of de Swart<sup>(13)</sup>, and Dalitz<sup>(14)</sup>.

We have observed 1  $\Sigma^+ \rightarrow \Lambda^0 + e^+ + \nu$  and 8  $\Sigma^- \rightarrow \Lambda^0 + e^- + \nu$  events in a scan of all 280'000 pictures. Using the number of  $\Lambda^0 e^- e^+$  events in these pictures and applying the same corrections for sigmas eliminated by length criteria, the effective number of  $\Sigma^+ \rightarrow \pi^+ + n$  and in  $\Sigma^- \rightarrow \pi^- + n$  decays is  $0.82 \times 10^5$  and  $3.3 \times 10^5$  respectively. We estimate the scanning efficiency for these events to be  $80 \pm 20$  percent of that for  $\Lambda^0 e^- e^+$  events.

1948

1948

1948

1948

1948

1948

1948

1948

1948

1948



The branching ratios are then

$$R_{\Lambda^-} = \frac{10 (1.56)}{0.8 (3.1 \times 10^5)} = 0.6 \pm 0.3 \times 10^{-4} \quad \text{and} \quad (4)$$

$$R_{\Lambda^+} = \frac{1 (1.56)}{(0.8) (0.82 \times 10^5)} \sim 0.2 \times 10^{-4}$$

If we identify the 3  $\Sigma^+ \rightarrow e^+$  events,  $P_{e^+}$  being smaller than 60 MeV/c, with the  $\Sigma^+ \rightarrow \Lambda e^+ \nu$ ,  $\Lambda \rightarrow n \pi^0$ , decay mode, we obtain

$$R_{\Lambda^+} = \frac{1 + 3 \times 1.135}{0.8 \cdot 0.82 \times 10^5} = 0.7 \pm 0.4$$

These values are in reasonable agreement with the predictions quoted above, given the limited statistics available.

#### Acknowledgements

We are indebted to the unflagging cooperation of the CERN PS and Saclay bubble chamber personnel throughout the run, and to the persistence and perspicacity of the scanning forces at Maryland, U.S. Naval Research Laboratory and CERN. We would like to thank for their invaluable help and support Mr. R. Engelmann, Dr. R. Florent, Prof. P. Franzini, Prof. B. Gregory, Mr. V. Hepp, Mr. E. Kluge and Dr. H. Schneider.

10-1-1

10-1-1

10-1-1

10-1-1

10-1-1

10-1-1

10-1-1

10-1-1

10-1-1

10-1-1

10-1-1

10-1-1

10-1-1

10-1-1

Footnotes

1. A. Barbaro-Galtieri, W.H. Barkas, H.H. Heckman, J.W. Patrick and F.H. Smith, Phys. Rev. Letters 9, 518 (1962).
2. W.E. Humphrey, J. Kirz, A.H. Rosenfeld and J. Leitner, p.442, and F. Crawford, Rapporteur's talk, p.827, Proc. of International High Energy Physics Conference, Geneva (1962).
3. L. Grimellini, T. Kikuchi, L. Lendinare, L. Monari and M.M. Block. Proc. of International High Energy Physics Conference, p. 457, Geneva (1962).
4. S. Barshay and R.F. Behrends: Phys. Rev. 114, 931 (1959), and S. Iwo and J. Leitner, Nuovo Cimento 22, 904 (1961).
- 4a. An experimental value of the  $\Sigma^\pm \longrightarrow \pi^\pm + n + \gamma$  can be derived from the two positive and the one negative we have observed.  
 We obtain  $\frac{\Sigma^+ \longrightarrow \pi^+ + n + \gamma}{\Sigma^+ \longrightarrow \pi^+ + n} \sim 0.4 \times 10^{-4}$ ,  
 and  $\frac{\Sigma^- \longrightarrow \pi^- + n + \gamma}{\Sigma^- \longrightarrow \pi^- + n} \sim 0.1 \times 10^{-4}$ ,  
 for  $\pi^\pm$  stopping inside the chamber and with a momentum  $p_{\pi^\pm} \approx 80$  MeV/c.
5. e.g. D.R. Harrington, Phys. Rev. 120, 1482 (1960). The curve drawn in Fig. 1 corresponds to setting the effective vector and axial vector coupling constants equal to each other ignoring all magnetic or induced pseudoscalar terms. This is essentially the same as phase space. The  $\mu^-$  spectrum is then transformed from the  $\Sigma^-$  rest system to the laboratory system, using  $\bar{p}_{\Sigma^-} = 155$  MeV/c. The differences in the  $\mu^-$  spectrum for different strengths of coupling are negligibly small when compared with the statistical accuracy of this experiment.
6. The probability of a  $\mu^-$  stopping in the chamber was estimated by taking a sample of  $K^-$  stopping points (these  $K^-$  gave rise to  $e^- + e^+ + \Lambda^0$ ) and calculating the potential range of  $\mu^-$  mesons versus momentum for a large selection of initial directions. The results of these calculations were combined to give the probability of a  $\mu^-$  stopping in the chamber as a function of its initial momentum.
7. W.E. Humphrey and R.R. Ross, Phys. Rev. Letters 127, 1305 (1962).
8. R.P. Ely, G. Gidal, G.E. Kalnus, L.O. Oswald, W.M. Powell, W.F. Singleton, F.W. Bullock, C. Henderson, D.S. Miller and R.R. Stannard, UCRL-10678, Phys. Review to be published.
9. The attempt to fit the ordinary hypothesis  $\Sigma^+ \longrightarrow \pi^+ + n$  gave a chi squared of 70 for one degree of freedom.

The first part of the document discusses the importance of maintaining accurate records of all transactions. It emphasizes that every entry should be supported by a valid receipt or invoice to ensure transparency and accountability.

Furthermore, it is noted that regular audits are essential to identify any discrepancies or errors in the accounting system. This process helps in maintaining the integrity of the financial data and ensures compliance with relevant regulations.

In addition, the document highlights the need for clear communication between all stakeholders involved in the financial process. Regular meetings and reports should be conducted to keep everyone informed about the current financial status and any upcoming challenges.

It is also stressed that the financial team should always stay updated with the latest market trends and economic indicators. This knowledge is crucial for making informed decisions and adjusting the financial strategy accordingly.

The document concludes by stating that a strong financial foundation is key to the long-term success of any organization. By following these guidelines, the company can ensure its financial health and stability in the future.

Finally, it is recommended that the financial records be reviewed and approved by the management team at regular intervals. This step is vital for ensuring that all financial activities are in line with the company's overall goals and objectives.

10. T. D. Lee and C.N. Yang, Phys. Rev. 119, 1410 (1960).
11. S. Weinberg, Phys. Rev. 112, 1375 (1958).
12. J. Dreitlein and H. Primakoff, Phys. Rev. 125, 1671 (1962).
13. J.J. de Swart, Physics Letters 5, 58 (1963).
14. R.H. Dalitz, Physics Letters 5, 53 (1963).

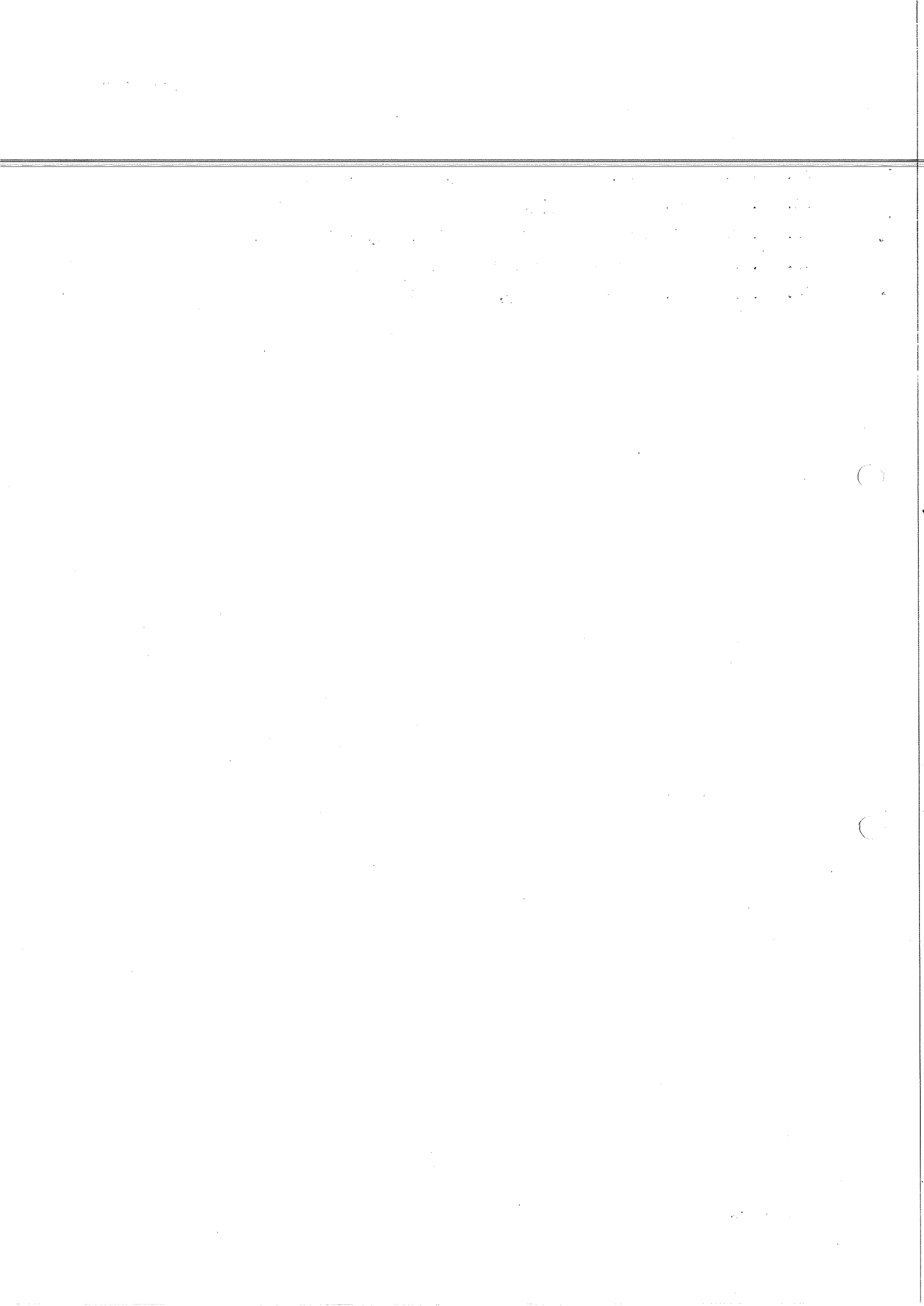




Figure Captions

Fig. 1 Histogram of the momentum distribution of 36 observed  $\Sigma^- \rightarrow \mu^- + n + \nu$  events. The 20 events where the  $\mu^-$  stops in the chamber are cross hatched. The lower smooth curve represents the calculated probability of obtaining stopping  $\mu^-$  events in the chamber multiplied by the phase space distribution in the laboratory system (upper smooth curve). Class a) of the events are pure  $\Sigma^- \rightarrow \mu^- + n + \nu$  events, while b) and c) contain also radiative  $\Sigma^-$  decays,  $\Sigma^- \rightarrow \pi^- + n + \gamma$ . In addition, class c) contains  $\mu^-$  from the reactions  $\Sigma^- \rightarrow \pi^- + n$ ,  $\pi^- \rightarrow \mu^- + \nu$ , where the  $\pi$  track is too short to be seen.

Fig. 2 Histogram of the momentum distribution of 68 observed  $\Sigma^- \rightarrow e^-$  decays. The upper smooth curve represents the calculated non-covariant phase space distribution of the electron momentum for the decay  $\Sigma^- \rightarrow e^- + n + \bar{\nu}$ , and the lower one for the decay  $\Sigma^- \rightarrow e^- + \Lambda^0 + \bar{\nu}$ . Both curves and the histogram are normalized to the sample a) of low momentum electrons. (Scanning for high momentum electrons is not yet complete).

Table I Table of  $\Sigma$  decay branching ratios.

100-100000-1000

100-100000-1000

100-100000-1000

100-100000-1000

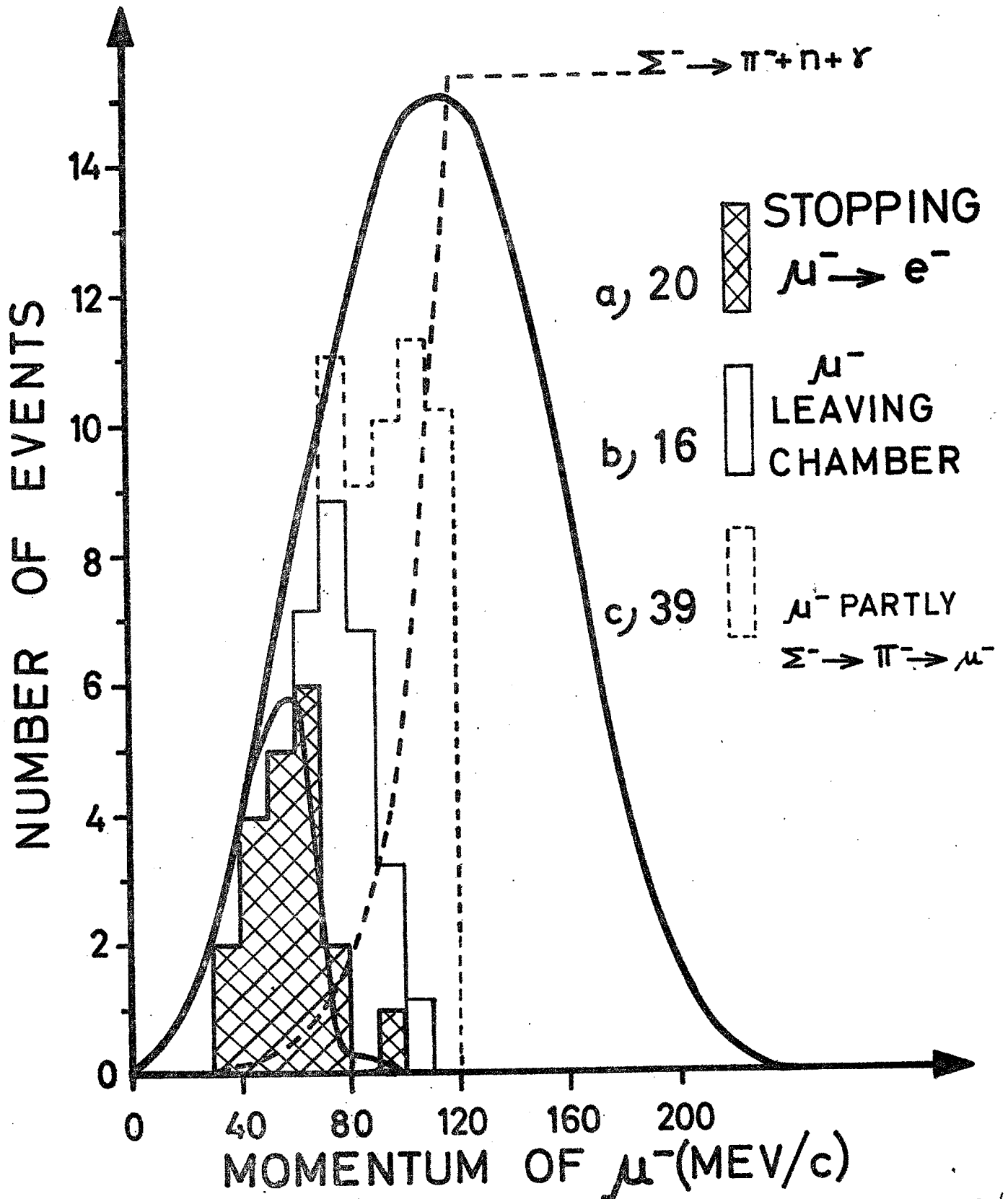
100-100000-1000

100-100000-1000

100-100000-1000



FIG. 1



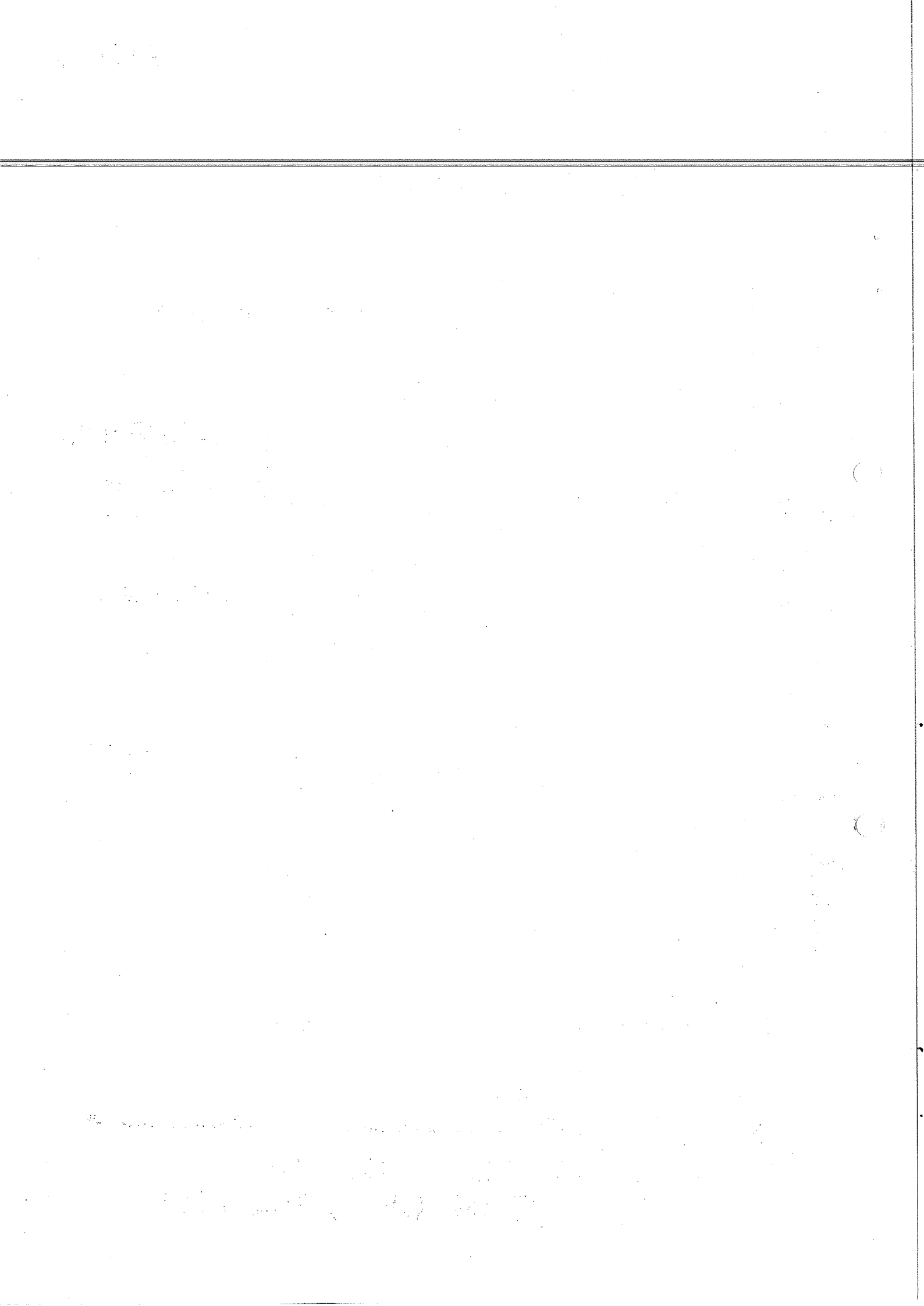
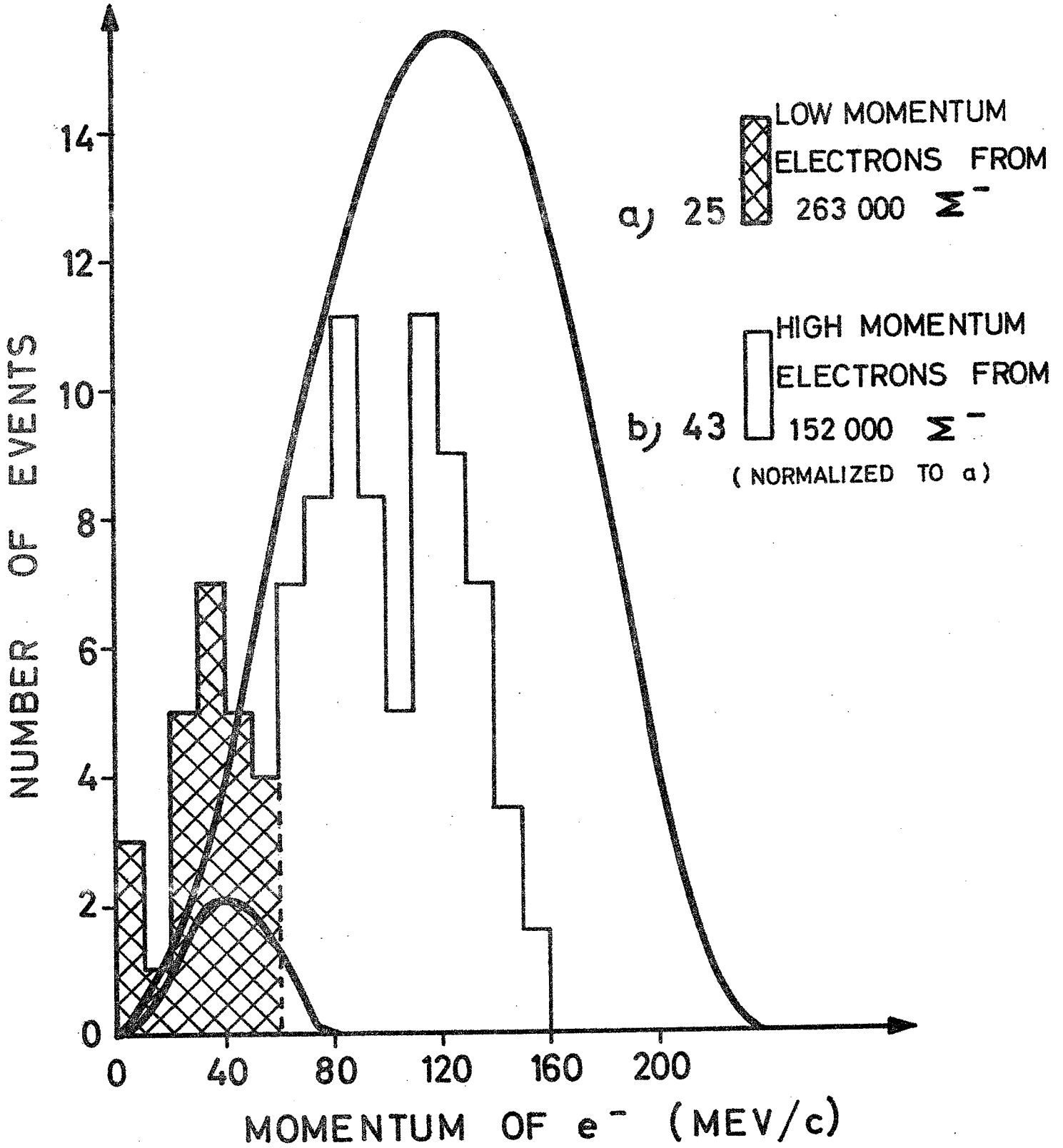


FIG. 2



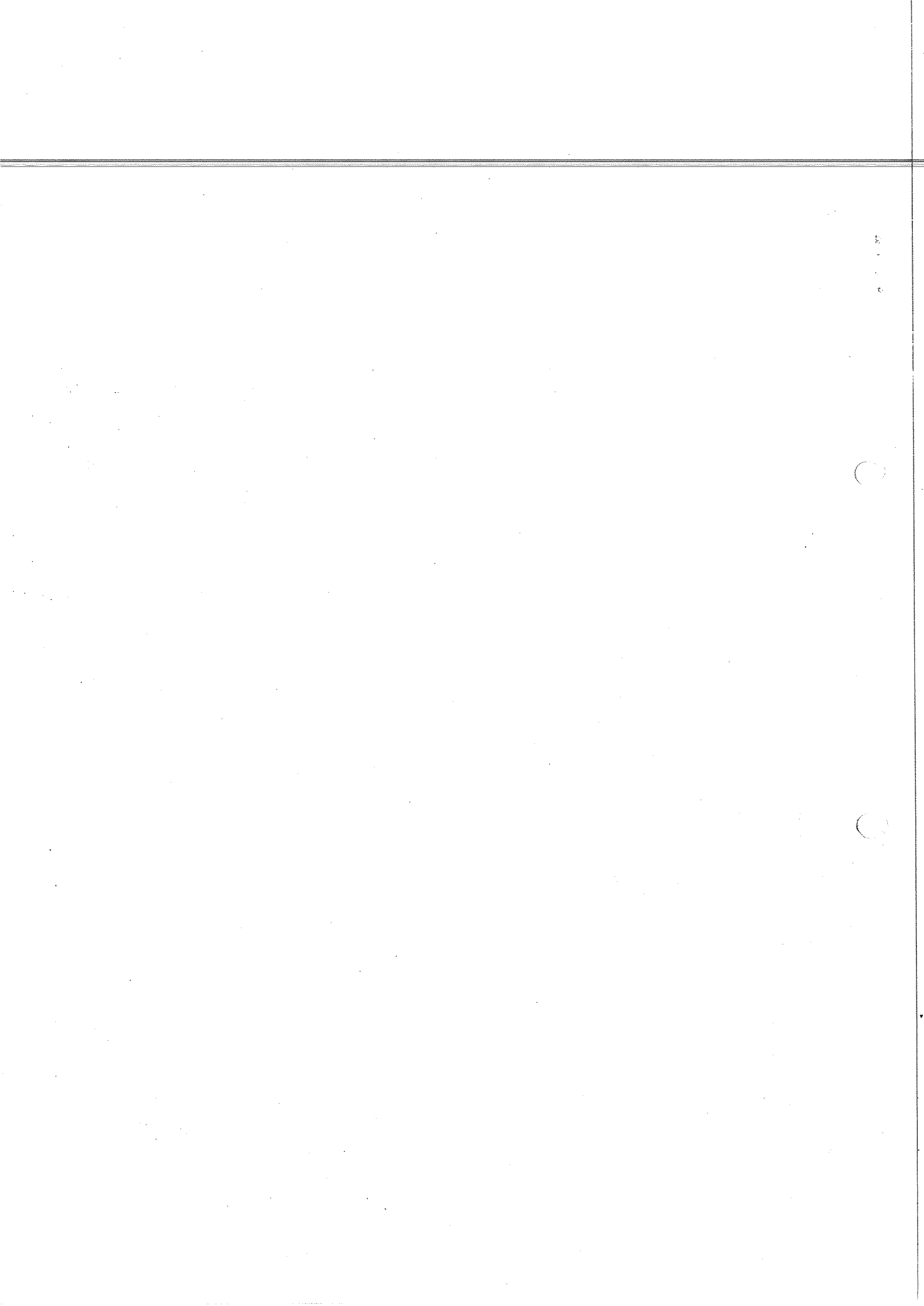


Table 1

| DECAY  | $R = \frac{\Sigma \rightarrow \text{LEPT.}}{\Sigma \rightarrow \pi}$ | No. of Events<br>$\Sigma \rightarrow \text{LEPT.}$                       | No. of DECAYS<br>$\Sigma \rightarrow \pi$ |                                |
|--|--|--|---|--------------------------------|
| $\Sigma^- \rightarrow e^- + n + \bar{\nu}$       | $(13 \pm 4) \times 10^{-4}$  | 21 ( $p_e \leq 50 \text{ MeV/c}$ )                                       | $47.6 \times 10^4$                        |                                |
| $\Sigma^- \rightarrow \mu^- + n + \bar{\nu}$     | $(8.8 \pm 3.0) \times 10^{-4}$                                       | 18 ( $\mu^-$ stop)   | $27.5 \times 10^4$                        |                                |
| $\Sigma^+ \rightarrow e^+ + n + \nu$             | $< 2.7 \times 10^{-4}$   | 0  | $11.1 \times 10^4$                        | to 90% confidence              |
| $\Sigma^+ \rightarrow \mu^+ + n + \nu$           | $< 4.0 \times 10^{-4}$   | 0  | $11.1 \times 10^4$                        | to 90% confidence              |
| $\Sigma^- \rightarrow \Lambda + e^- + \bar{\nu}$ | $(0.6 \pm 0.3) \times 10^{-4}$                                       | 10 ( $\Lambda \rightarrow p\pi^-$ )                                      | $47.6 \times 10^4$                        |                                |
| $\Sigma^+ \rightarrow \Lambda + e^+ + \nu$       | $(0.7 \pm 0.4) \times 10^{-4}$                                       | 1 ( $\Lambda \rightarrow p\pi^-$ )<br>3 ( $\Lambda \rightarrow n\pi^0$ ) | $11.1 \times 10^4$                        |                                |
| $\Sigma^- \rightarrow \pi^- + n + \gamma$        | $\sim 0.1 \times 10^{-4}$  | 1  | $27.5 \times 10^4$                        | For $p_\pi < 80 \text{ MeV/c}$ |
| $\Sigma^+ \rightarrow \pi^+ + n + \gamma$        | $\sim 0.4 \times 10^{-4}$  | 2  | $6.4 \times 10^4$                         | For $p_\pi < 80 \text{ MeV/c}$ |

